Simultaneous Reduction and Polymerization of Graphene Oxide/Styrene Mixtures to Create Polymer Nanocomposites with Tunable Dielectric Constants

Dandan Hou,[a,b,c,†] Joshua E. Bostwick,[a,†] Jeffrey R. Shallenberger,[d] Everett S. Zofchak,[a,e] Ralph H. Colby,[a,d] Qinfu Liu,[b] Robert J. Hickey[a,d,*]

[a]Department of Materials Science and Engineering, The Pennsylvania State University, University Park, Pennsylvania 16802, United States
[b]College of Geoscience and Surveying Engineering, China University of Mining and Technology, Beijing, 100083, China
[c]School of Electronics Engineering and Computer Science, The Peking University, Beijing, 100871, China
[d]Materials Research Institute, The Pennsylvania State University, University Park, Pennsylvania 16802, United States
[e]Department of Chemical Engineering, The Pennsylvania State University, University Park, Pennsylvania 16802, United States

* Corresponding e-mail: rjh64@psu.edu
† Authors contributed equally

Abstract

Polymer nanocomposites containing carbon nanomaterials such as carbon black, carbon nanotubes, and graphene exhibit exceptional mechanical, thermal, electrical, and gas barrier properties. Although the materials property benefits are well established, controlling the dispersion of carbon nanomaterials in polymer matrices during processing is still a difficult task using current methods. Here, we report a simple, yet versatile method to simultaneously achieve the reduction of graphene oxide (GO) and polymerization of styrene to create reduced graphene oxide/poly(styrene) (RGO/PS) nanocomposite materials *via* microwave heating. The RGO/PS mixture is then processed into films of desired thicknesses by first removing unreacted styrene and then pressing the powder at elevated temperatures. X-ray photoelectron spectroscopy (XPS) indicated that microwave processing was able to reduce GO, which resulted in a change in the carbon to oxygen ratio (C/O) from 2.0 of GO to 4.5 for RGO. Furthermore, the addition of GO in the RGO/PS nanocomposites lead to an increase in the static dielectric constant (ε_s) relative to pure PS, with

minimal change in tan δ (~0.06% at room temperature). The simultaneous microwave reduction/polymerization method described here will potentially lead to the production of polymer-based dielectric nanocomposite materials with tunable dielectric constants for energy storage applications.

Keywords: reduced graphene oxide, polymer nanocomposites, microwave synthesis, dielectric constant, dielectric relaxation spectroscopy

Introduction

Graphene-based polymer nanocomposites have attracted significant attention from the polymer and nanomaterial communities in recent years due to their excellent electrical,[1,2] mechanical,[3,4] and gas barrier properties.[5,6] The superior properties that arise from dispersing carbon-based nanomaterials such as graphene, graphene oxide (GO), and reduced graphene oxide (RGO) within polymer matrices are produced through a combination of the inherent physical properties of graphene (*e.g.*, high electrical and thermal conductivity)[7,8] and the geometric shape.[9] For example, well-dispersed anisotropic atomistically-thin two-dimensional (2D) RGO nanosheets are able to prevent crack propagation within epoxy nanocomposites, increasing the fracture toughness of the materials.[9] On the other hand, RGO/epoxy nanocomposites in which the RGO nanosheets are aggregated exhibited significantly reduced electrical conductivity as compared to the well-dispersed samples.[9] The enhanced properties of graphene-based polymer nanocomposites are ultimately controlled by the level of dispersion and orientation of the carbon nanofillers,[9,10] and by judicious selection of the chemical and architectural composition of the polymer matrix in order to maximize the interfacial interactions between the filler and the polymer.[3,4,6,11,12] With the vast array of synthetic and processing techniques available to researchers, much still remains to be explored with respect to tailoring the physical properties of graphene-based polymer nanocomposites, as well as finely tuning the nanostructure of the materials.

When preparing graphene-based polymer nanocomposites, three techniques are commonly employed: *in situ* polymerization, solution blending, and melt blending.[13,14] While *in situ* methods in many cases lead to more uniform dispersion of the graphene, GO, and RGO nanofillers,[4,15,16] the latter two processing techniques are more commonly used in industry due to the economic

benefits and scalability.[13] In many of the polymer nanocomposite preparation methods, harsh chemical reagents like hydrazine hydrate are used to remove (reduce) the oxygen-containing functional groups (*e.g.*, epoxide, carbonyl, hydroxyl, phenol) from GO during fabrication.[17,18] For these reasons, many have explored using less hazardous chemical reduction processes to form RGO by thermal treatments,[19,20] microwave processes,[21] or green syntheses.[22-24] From an environmental perspective, processes that utilize the convenient, rapid, and uniform heating that simultaneously reduces GO while maintaining dispersion in polymer matrices are highly desirable.

Graphene-based polymer nanocomposite materials created using *in situ* polymerization procedures have shown to increase graphene, RGO, and GO dispersion within polymer matrices, and lead to enhanced mechanical and electrical properties.[10,16,25,26] One method in particular, microwave heating, to simultaneously reduce GO and synthesize polymers has been shown to be an efficient method for creating polymer nanocomposites with well-dispersed RGO.[25,27,28] Microwave heating has been broadly applied to many chemical reactions ranging from organic syntheses to polymerization due to increased product yields and reaction rates.[29,30] For example, as compared to conventional heating, microwave-assisted synthesis of poly(styrene) has been shown to reduce reaction times.[31,32] Furthermore, microwave-assisted polymer grafting on diblock copolymers to induce nanostructural transitions have been recently reported,[33] suggesting that the combination of nanoscale fillers with polymer materials using microwave reaction processes will lead to advances in the creation of nanostructured hybrid polymer materials. Therefore, the combination of microwave heating to simultaneously polymerize monomer and reduce GO has major benefits for rapidly producing RGO polymer nanocomposites. Previous results indicate that it is possible to reduce GO during microwave heating with hydrazine hydrate to create polymer nanocomposites

with improved hardness and elastic modulus.[25] Although the increase in the mechanical properties of RGO/polymer nanocomposites are of interest, the electrical property enhancement of graphene-based composites fabricated using microwave heating will potentially lead to advancements in energy storage applications.[34,35] Furthermore, microwave heating has been shown to be an effective method for completely reducing GO to pristine graphene.[21] Therefore, by combining microwave heating to simultaneously reduce GO without chemical reducing reagents and polymerize polymers using controlled radical polymerization methods,[31,36-39] it will be possible to rapidly create graphene-based polymer nanocomposite materials with tunable physical properties.

The simultaneous reduction of GO and polymerization of monomer using microwave heating to produce hybrid polymer materials for dielectric polymer capacitor films is an exciting area with enormous potential in energy storage.[40] Polymeric films need to exhibit a combination of a high dielectric constant (ε_s), a low dissipation factor (tan δ), and a wide temperature window to be properly implemented for dielectric capacitors.[35] To this end, researchers have investigated incorporating RGO as a conductive filler in polymer matrices and its effect on dielectric properties.[41-44] While these studies have been able to produce enhanced dielectric constants with increasing RGO content into the matrix, they also lead to an elevated dissipation factor in the film, which is likely due to the low glass transition temperature (T_g) of the polymer matrix. By introducing RGO into polymer matrices exhibiting low T_g, RGO fillers are able to form a percolating network, leading to an increase in the dissipation factor.[40] As a result, tan δ increases, reducing the material's effectiveness in capacitor applications. Therefore, it is imperative to investigate the effects of RGO, or additional nanoscale fillers, in polymer matrices with elevated T_g in order to increase ε_s while maintaining low tan δ for uses in high-energy-density storage

dielectric capacitors.[34,45-49]

Here, in an effort to address the elevated dissipation factor in RGO nanocomposite materials in previously reported work using low T_g polymers, we report the simultaneous reduction of GO and the nitroxide-mediated polymerization (NMP) of styrene to form RGO/poly(styrene) (PS) nanocomposites with varying weight percent of GO. PS is a model polymer for studying the dielectric and dissipative properties in RGO nanocomposite materials due to the much higher T_g as compared to previous low T_g polymers. Transmission electron microscopy (TEM) images reveal that the microwave process to produce RGO/PS nanocomposite materials described here results in well-dispersed RGO in the PS matrix, and the materials exhibit increased dielectric constants and low tan δ. The static dielectric constant of the RGO/PS nanocomposites synthesized increased with increasing GO content, which is attributed to increasing the content of a higher dielectric constant material, such as RGO. Moreover, the RGO-containing polymer nanocomposites exhibit low loss values that are similar to commercially used polymer materials. The microwave processing method described here to achieve RGO/PS nanocomposite materials has potential applications in dielectric polymer nanocomposite materials.

Experimental

Materials and methods

Graphite powder (Shandong Nanshu Graphite Ore Co., Ltd., China) was converted to graphite oxide following a modified Hummers method,[50] and dried at 50 °C for 12 h. Styrene (≥ 99%), benzoyl peroxide (BPO, 98%), and 4-hydroxy-2,2,6,6-tetramethylpiperidine (OH-TEMPO, 97%) were purchased from Sigma-Aldrich.

Preparation of RGO/PS nanocomposites

The synthetic procedure for creating RGO/PS polymer nanocomposites is shown in **Figure 1**. First, a desired amount of GO powder was dispersed in 20 mL styrene (the inhibitor in styrene was removed by passing styrene through basic alumina) and was sonicated for 1 h to form GO/styrene suspensions at various concentrations (0.05, 0.1, 0.25, 0.5, 1, 2.5 wt% of GO in styrene). Next, BPO (0.01421 g) and OH-TEMPO (0.0067 g) where added to the GO/styrene suspensions. The reduction and polymerization of GO and styrene, respectively, was performed under microwave radiation for 3 h at 200 °C and 100 W using a Discover LabMate with IntelliVent pressure and infrared temperature control system (CEM Co.) in dynamic power mode. Note, the CEM Co. Discover LabMate with IntelliVent pressure device can manage reactions at temperatures above the boiling point of solvents and monomers like styrene (*e.g.*, b.p. 145 °C). After the microwave reaction, the mixture was cooled to room temperature, and unreacted styrene was removed by applying dynamic vacuum for 4 h at 120 °C. Finally, the RGO/PS nanocomposite powder was fabricated into films using a vacuum mold pressing instrument (105 °C for 10 min). As shown in **Figure 1**, the film (~0.15 mm) containing 2.5 wt% GO is black and opaque.

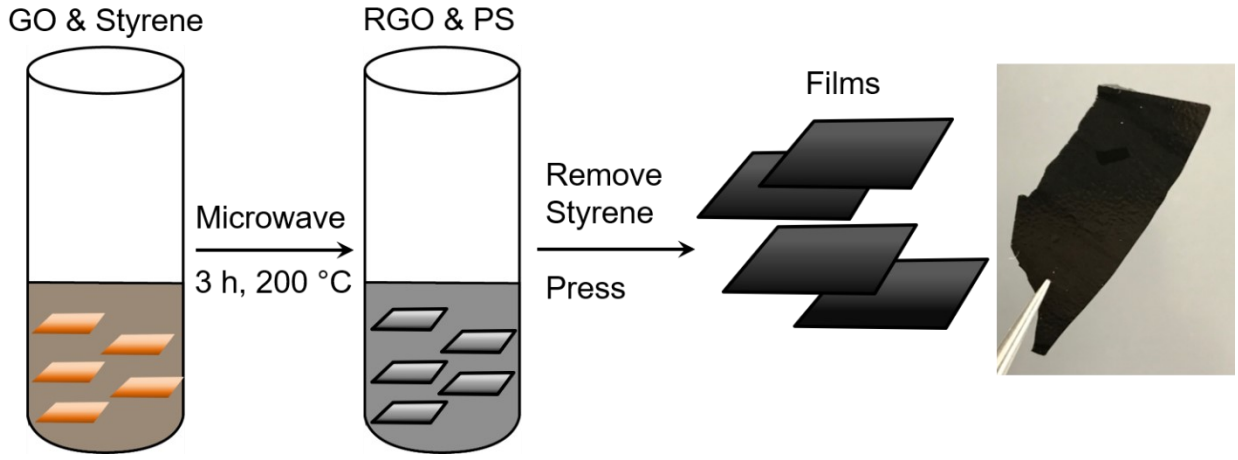

Figure 1. Overview of the synthetic and processing method for the preparation of RGO/PS polymer nanocomposites. As seen in the digital photograph on the right, RGO/PS polymer nanocomposites films (2.5 wt% GO) are easily obtained after thermal pressing. The image of the RGO/PS nanocomposite film shown on the right is 0.15 mm thick.

X-ray photoelectron spectroscopy (XPS)

X-ray photoelectron spectroscopy (XPS) experiments were performed using a Physical Electronics VersaProbe II instrument equipped with a monochromatic Al kα x-ray source (hv = 1,486.7 eV) and a concentric hemispherical analyzer. Charge neutralization was performed using both low energy electrons (<5 eV) and argon ions. The binding energy axis was calibrated using sputter cleaned Cu foil (Cu $2p_{3/2}$ = 932.7 eV, Cu $2p_{3/2}$ = 75.1 eV). Peaks were charge referenced to CH_x band in the carbon 1s spectra at 284.8 eV. Measurements were made at a takeoff angle of 45° with respect to the sample surface plane. This resulted in a typical sampling depth of 3 – 6 nm (95% of the signal originated from this depth or shallower). Quantification was done using instrumental relative sensitivity factors (RSFs) that account for the x-ray cross section and inelastic mean free path of the electrons.

Differential Scanning Calorimetry (DSC)

Glass transition temperatures (T_g) of the PS and RGO/PS polymer nanocomposites were determined using a PerkinElmer 8500 differential scanning calorimeter (DSC) under dry nitrogen purge. All samples were placed in vacuum oven for 80 °C for 24 h to remove residual moisture. Approximately 8 mg of sample was used as the sample size. Polymer samples were heated from room temperature to 140 °C and annealed for 30 min. After annealing at 140 °C, samples were

cooled to 20 °C, and then heated back to 140 °C. Cooling and heating rates were of 10 °C/min. The T_g was determined by the inflection point in the heat capacity change during the second heating cycle.

Transmission electron microscopy (TEM)

Two TEM sample preparation methods were used to characterize GO in solution and RGO in PS matrices. To characterize the lateral dimensions of GO before and after sonication (before polymerization), a solution of graphene oxide (0.5 wt% in toluene) was drop cast onto a carbon-copper grid before and after sonication (1 h). To characterize the RGO dispersion in PS, a 2.5 wt% RGO in PS film was microtomed into 70 – 90 nm sections using a Leica UC6 ultramicrotome. Samples were imaged using a FEI Tecnai G2 Spirit BioTwin TEM.

Dielectric Relaxation Spectroscopy (DRS)

Dielectric measurements of the PS and RGO/PS polymer nanocomposites were carried out by dielectric relaxation spectroscopy (DRS) using a Novocontrol GmbH Concept 40 broadband dielectric spectrometer. All samples were sandwiched between a polished 10 mm top brass electrode and a polished 30 mm brass electrode with thicknesses of the films ranging between 0.12 – 0.15 mm. The thicknesses were measured before and after measuring to ensure proper results. Each sample was loaded into the Novocontrol and annealed at 80 °C under nitrogen for an additional hour to remove any moisture picked up during sample loading. Isothermal dielectric data were then collected using a sinusoidal voltage with an amplitude of 1.5 V over a frequency range of 10^{-1} – 10^{7} Hz in steps of 10 °C on cooling from 80 °C to 0 °C followed by steps of 5 °C on heating from 0 °C to 80 °C to ensure the data were reproducible over the same frequency and

temperature range.

Results and Discussion

Synthesis of RGO/PS nanocomposite films

Reduced graphene oxide/poly(styrene) (RGO/PS) films of controlled thickness were produced by first simultaneously reducing and polymerizing GO and styrene, respectively, using microwave radiation (3 h at 200 °C and 100 W), and then thermally pressing the RGO/PS powder under vacuum after removal of unreacted styrene (**Figure 1**). Distinct color changes occurred in GO/styrene mixtures after microwave synthesis. For all GO/styrene mixtures, the color transitioned from brown to black, which is indicative of the removal of the oxygen-containing functional groups.[17] Neat PS samples were also produced using the same microwave reaction conditions, which is similar to previously published NMP results for the synthesis of PS.[38,39] The number-average and weight-average molecular weight (M_n and M_w), and dispersity ($Đ$) of the neat PS after microwave synthesis (3 h at 200 °C and 100 W) and vacuum drying was found to be 10.1 kg/mol, 14.3 kg/mol, and 1.42, respectively.

The reaction and processing procedures for creating RGO/PS nanocomposites was easily adaptable to incorporate varying amounts of RGO in the PS matrices (**Figure 2**). As seen in **Figure 2**, the pure PS film is transparent, but increasing GO in styrene, the appearance of the films transitioned from transparent and light gray to opaque and black. To control the amount of RGO in the PS matrices, different quantities of dried GO powder were dispersed in styrene in prescribed weight fractions *via* sonication prior to microwave radiation. Furthermore, the thermal pressing process allowed for the fabrication of RGO/PS nanocomposite films with relatively large areas and

uniform composition.

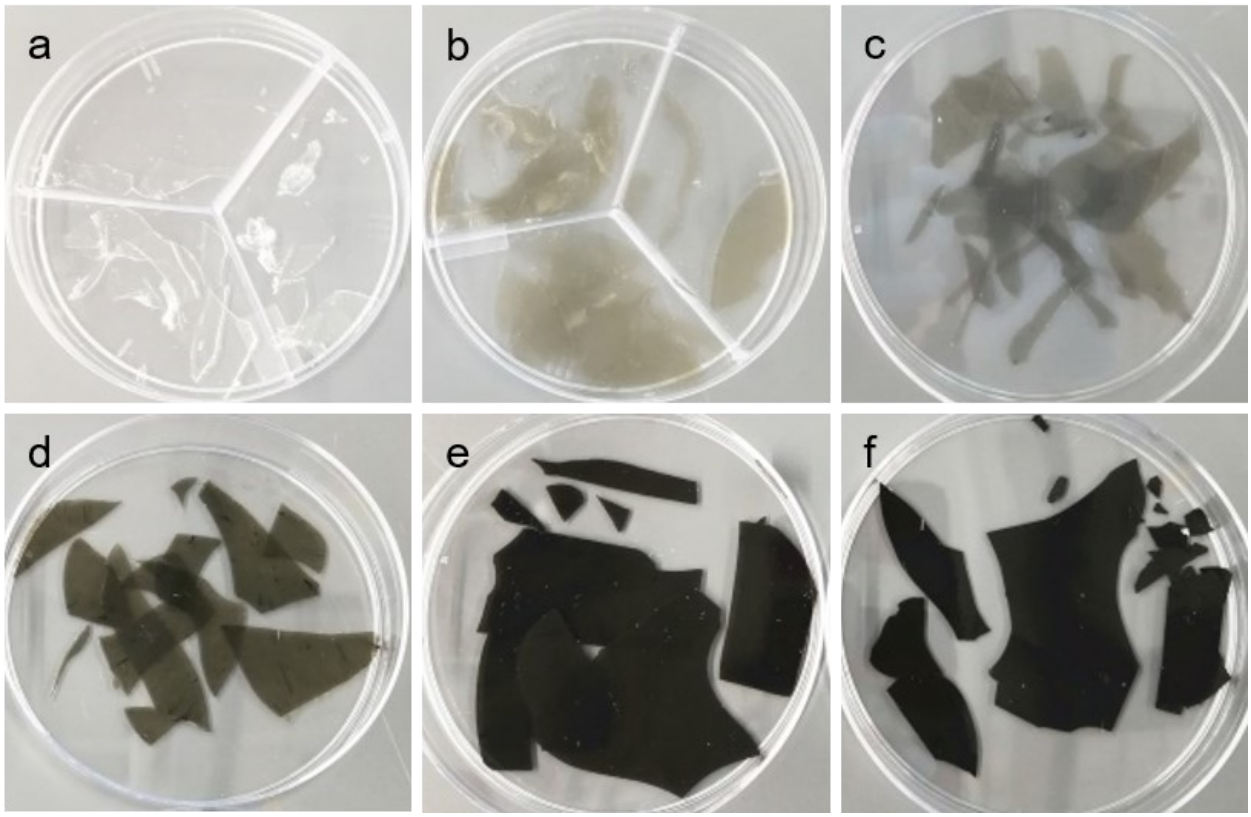

Figure 2. Images of pressed polymer and polymer nanocomposite films. RGO/PS nanocomposite materials containing (a) 0, (b) 0.05, (c) 0.25, (d) 0.5, (e) 1.0, and (f) 2.5 wt% GO. The polymer nanocomposite films become significantly darker with increasing RGO content.

X-ray photoelectron spectroscopy (XPS) analysis

To evaluate the reduction efficiency of GO using the microwave heating conditions described here, XPS was used to determine the carbon-to-oxygen ratio (C/O), which is a quantitative indicator of the reduction efficiency.[51] **Figure 3** shows the C 1s XPS spectra for GO and RGO before and after microwave heating, respectively, and of PS and 2.5 wt% RGO in PS after film processing. The GO

sample was the graphene oxide produced from the Hummers method, and the RGO sample was produced by microwave heating GO in deionized (DI) water (1 h at 200 °C and 100 W). The XPS analysis for the 2.5 wt% RGO in PS after film processing was chosen because it was either not possible or very hard to detect the graphitic signal using XPS signal for the RGO/PS samples with reduced RGO content.

The C 1s spectrum of GO often has characteristic peaks centered at the binding energy 284.8 eV, 286.2 eV, 287.8 eV, and 289.0 eV, which represent the C-C, C-O, C=O, O-C=O, respectively.[17,51] From fitting the spectra, it was found that after microwave treatment, the peaks representing C-O and C=O decreased dramatically, suggesting the removal of oxygen-containing functional groups. The C/O ratio of the GO we obtained was determined to be 2.0 by XPS, which is in agreement with previous studies.[17,51] After microwave treatment, the C/O ratio increased from 2.2 (GO) to 4.5 (RGO), demonstrating the successful de-oxygenation of GO by microwave heating. As for the 2.5 wt% RGO in PS after film processing, analysis of the O 1s spectrum indicates that there is minimal oxygen species (C/O ratio is 240), which correlates to a dilution of RGO in PS if the O content of the RGO is constant during polymerization. **Table 1** lists the experimentally determined C, O, and C/O ratios for GO, RGO, PS, and 2.5 wt% RGO in PS. Although the C/O ratio of RGO created by microwave heating shown here is not as efficient as standard chemical methods or microwave heating procedures, the process reported here is quicker, easier, and uses less hazardous chemicals to produce RGO/PS nanocomposite materials.[17] It is worth noting that the RGO created here is chemically different from as pure graphene, as there is still a considerable amount of oxygen-containing species on the RGO sheets, which is difficult to remove by microwave treatment using the procedure described here.

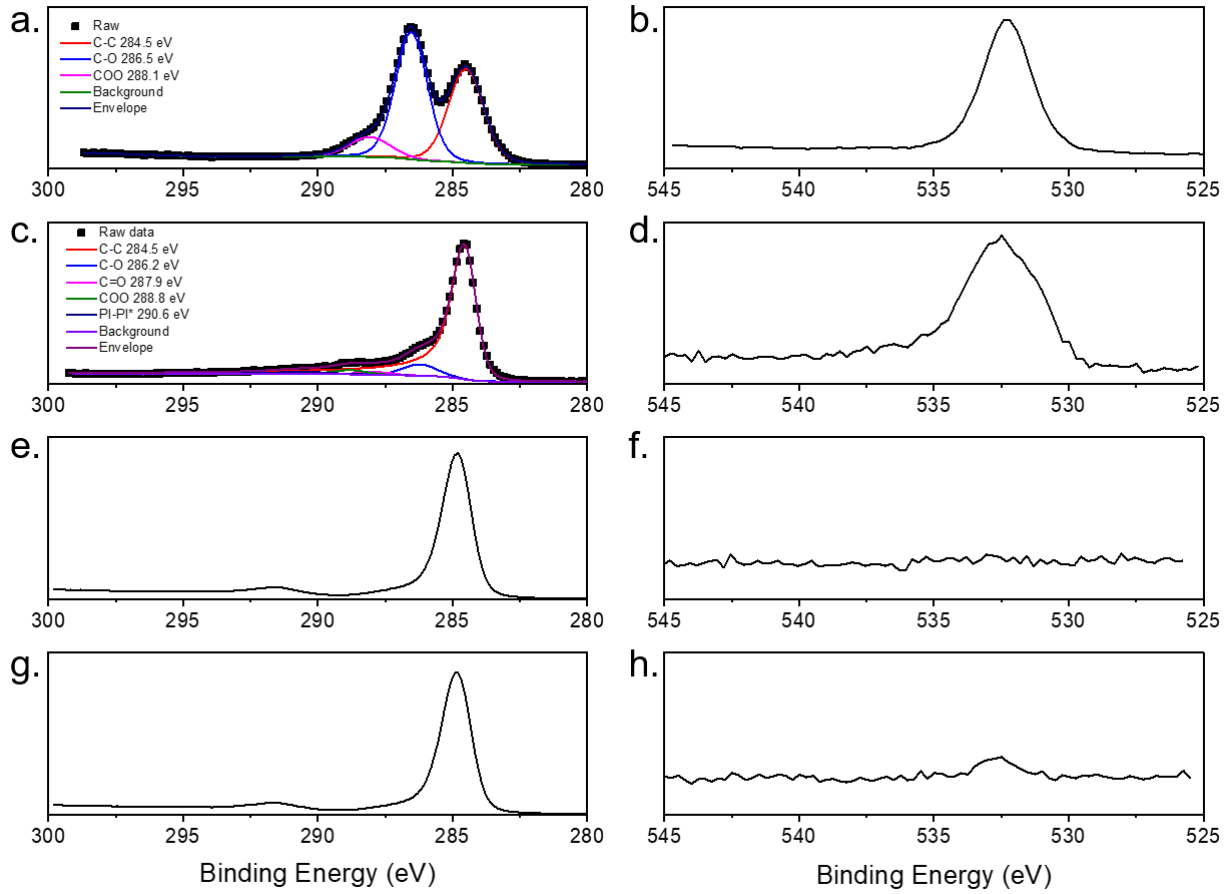

Figure 3. XPS C 1s (left side) and O 1s (right side) spectra for GO, RGO, PS, and 2.5 wt% RGO in PS. (a) Fitted XPS C 1s and (b) O 1s spectra for GO. (c) Fitted XPS C 1s and (d) O 1s spectra for RGO after microwave treatment of GO in water (1 h at 200 °C and 100 W). XPS C 1s and O 1s spectra for (e, f) PS and (g, h) 2.5 wt% RGO in PS.

Table 1. C, O, and C/O ratio for GO, RGO, PS, and 2.5 wt% RGO in PS

Carbon Containing Species	GO	RGO	PS	2.5 wt%
Total C	66.8	81.8	100.0	99.6
Total O	33.2	18.2	NA	0.4
C/O ratio	2.0	4.5	NA	240

Thermal and Structural Characterization

To understand how the glass transition temperature changes as a function of GO content, we used differential scanning calorimetry (DSC) and analyzed the change in heat capacity. The T_g values for four different samples (RGO content: 0, 0.05, 0.5, and 2.5 wt% in PS) are listed in **Table 2**. All four samples show similar T_g values (range: 82.0 – 87.5 °C), which is less than the T_g value for bulk PS.[52] The reduction in T_g for the four samples in **Table 2** is hypothesized to be due to the processing method, which leaves oligomeric PS species in the sample that are not removed during vacuum drying. This claim is supported by the fact that PS samples produced using the same microwave heating process described here exhibit $T_g \approx 101$ °C when precipitated in methanol, vacuum dried, and run using DSC (Note: the molecular weight of the PS samples processed using different procedures (*e.g.*, vacuum dried *vs* precipitated have similar molecular weights as shown in **Tables 2** and **S1**.)). Oligomeric PS species will plasticize the PS materials, reducing the overall T_g.

Table 2. Molecular and thermal characterization for polymer samples containing varying amounts of RGO[a]

RGO wt%	M_n (kg/mol)	M_w (kg/mol)	$Đ$	T_g (°C)
0	10.1	14.3	1.42	82.0
0.05	14.4	17.0	1.18	86.0
0.5	17.6	22.4	1.27	87.5
2.5	25.2	35.2	1.40	84.2

[a]Molecular weights and dispersities ($Đ$) were determined using a Tosoh EcoSEC (Tosoh Co.) equipped with a Wyatt Dawn Heleos-II eight angle light scattering detector (Wyatt Technology Corp.) using in tetrahydrofuran as the mobile phase at 40 °C.

Previously published results suggest that the decrease in the RGO/PS nanocomposites is due to non-uniform dispersion of RGO in the polymer matrix.[25] That is not the case here. TEM images of the 2.5 wt% RGO in PS indicate that the RGO is well-dispersed in the PS matrix (**Figure 4**).

The major difference in the system shown here is that the TEM images suggest that the RGO either reduces in size or clumps up during the microwave heating. The TEM images of GO before and after sonication show no noticeable change in the lateral dimensions of GO. After 3 h microwave heating, the RGO is significantly reduced in dimension. In all, the reduced T_g is hypothesized to result in residual oligomeric PS species in the samples, not microstructural contributions such as RGO aggregation.

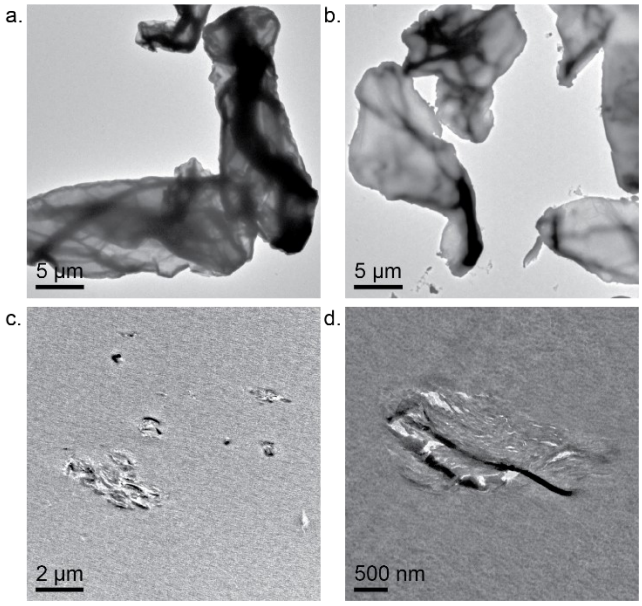

Figure 4. TEM images of GO and RGO/PS nanocomposites. Images of GO (a) before and (b) after sonication in toluene. GO was sonicated in toluene for 1 h, similar to the sonication procedure for preparing GO/styrene mixtures before microwave. (c, d) TEM images of microtomed RGO/PS nanocomposite films containing 2.5 wt% RGO.

Dielectric Constant and Dissipation Factor of RGO/PS Films

Utilizing DRS allows for the precise measurement of the static dielectric constant (ε_s) of polymeric materials, which is of significant importance for polymer film capacitors.[53] Typically, ε_s is

determined from the low frequency plateau of the real part of permittivity (ε') prior to electrode polarization (EP).[54,55] However, due to all of the measurements occurring at temperatures below the T_g of the PS and RGO/PS nanocomposites, no EP was detected and $\varepsilon' \approx \varepsilon_s$, which is similar to what has been previously shown in polymer nanocomposite materials for samples below T_g.[56] To illustrate this, **Figure 5** shows the temperature dependence of the permittivity for the PS and RGO/PS nanocomposites. As the GO content increased in the nanocomposite, ε' reaches a maximum value of 3.14 at room temperature which is greater than neat polymers that have been incorporated for capacitor use such as polycarbonate (PC, 2.8), polypropylene (PP, 2.2), and polyphenylene sulfide (PPS, 3.0).[57] While it appears that ε_s reaches a saturation limit with increasing GO content, it is expected that the ε_s will decrease with further increases in GO content, which has been previously reported in nanocomposite systems.[56] In the work presented here, the highest GO loading possible was 2.5 wt% due to the minimal solubility of GO in styrene.

In addition to increasing the dielectric constant of the RGO/PS nanocomposites with increase RGO content, there is minimal change in the loss ($tan\ \delta = \frac{\varepsilon''}{\varepsilon'}$) at constant temperature (**Figure 5**). Furthermore, there is an increase in tan δ for PS and the RGO/PS nanocomposites with increasing temperature. The increase in tan δ is due to the RGO/PS nanocomposites approaching T_g. However, while tan δ increases with increasing GO content, the value is never greater than ~0.06% at room temperature, which is comparable to polymeric systems currently used for capacitor applications.[57]

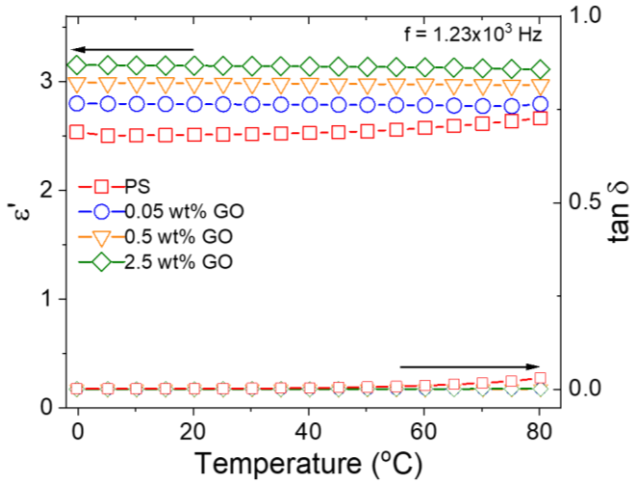

Figure 5. Temperature dependence on the static dielectric constant and tan δ of RGO/PS nanocomposite materials. Isochronal temperature dependence of the real permittivity (ε') and the dissipation factor (tan δ) as a function of temperature of PS and RGO/PS polymer nanocomposite films at a fixed frequency (1.23 kHz).

Conclusion

The work reported here describes a microwave heating method to create RGO/PS polymer nanocomposites by simultaneously reducing and polymerizing a GO/styrene mixture. The RGO/PS nanocomposite materials were processed into films of desired thicknesses by vacuum pressing powdered samples at elevated temperatures. The RGO/PS polymer nanocomposites exhibited greater static dielectric constants as compared to neat PS, which is attributed to the addition of a higher dielectric constant filler into the polymer matrix. The simultaneous reduction-polymerization process described here has potential applications for facile synthesis and processing of dielectric materials for energy storage applications.

ASSOCIATED CONTENT

Supporting Information

The Supporting Information is available free of charge *via* the Internet at http://pubs.acs.org. Additional data include SEC traces and tabulated polymer molecular characteristics.

AUTHOR INFORMATION

Corresponding Author

*E-mail: rjh64@psu.edu

ORCID

Robert J. Hickey: 0000-0001-6808-7411

Notes

The authors declare no competing financial interest.

ACKNOWLEDGMENTS

This work was supported by the National Science Foundation, Division of Materials Research Polymers Program (DMR-1807934), start-up funds from the Penn State University, the National Natural Science Foundation of China (41672150), the China Scholarship Council, the PPG/MRI Undergraduate Fellowship, and the Erickson Discovery Grant. XPS measurements and TEM were taken at the Materials Characterization Lab (MCL) in the Materials Research Institute (MRI) at the Penn State University.

REFERENCES

(1) Kim, K. S.; Zhao, Y.; Jang, H.; Lee, S. Y.; Kim, J. M.; Kim, K. S.; Ahn, J.-H.; Kim, P.; Choi, J.-Y.; Hong, B. H. Large-scale pattern growth of graphene films for stretchable transparent electrodes. *Nature* **2009**, *457*, 706.

(2) Petrone, N.; Meric, I.; Hone, J.; Shepard, K. L. Graphene Field-Effect Transistors with Gigahertz-Frequency Power Gain on Flexible Substrates. *Nano Lett.* **2013**, *13*, 121-125.

(3) Compton, O. C.; Cranford, S. W.; Putz, K. W.; An, Z.; Brinson, L. C.; Buehler, M. J.; Nguyen, S. T. Tuning the Mechanical Properties of Graphene Oxide Paper and Its Associated Polymer Nanocomposites by Controlling Cooperative Intersheet Hydrogen Bonding. *ACS Nano* **2012**, *6*, 2008-2019.

(4) Naebe, M.; Wang, J.; Amini, A.; Khayyam, H.; Hameed, N.; Li, L. H.; Chen, Y.; Fox, B. Mechanical Property and Structure of Covalent Functionalised Graphene/Epoxy Nanocomposites. *Sci. Rep.* **2014**, *4*, 4375.

(5) Morimune, S.; Nishino, T.; Goto, T. Ecological Approach to Graphene Oxide Reinforced Poly (methyl methacrylate) Nanocomposites. *ACS Appl. Mater. Interfaces* **2012**, *4*, 3596-3601.

(6) Compton, O. C.; Kim, S.; Pierre, C.; Torkelson, J. M.; Nguyen, S. T. Crumpled Graphene Nanosheets as Highly Effective Barrier Property Enhancers. *Adv. Mater.* **2010**, *22*, 4759-4763.

(7) Mayorov, A. S.; Gorbachev, R. V.; Morozov, S. V.; Britnell, L.; Jalil, R.; Ponomarenko, L. A.; Blake, P.; Novoselov, K. S.; Watanabe, K.; Taniguchi, T.; Geim, A. K. Micrometer-Scale Ballistic Transport in Encapsulated Graphene at Room Temperature. *Nano Lett.* **2011**, *11*, 2396-2399.

(8) Balandin, A. A.; Ghosh, S.; Bao, W.; Calizo, I.; Teweldebrhan, D.; Miao, F.; Lau, C. N. Superior Thermal Conductivity of Single-Layer Graphene. *Nano Lett.* **2008**, *8*, 902-907.

(9) Tang, L.-C.; Wan, Y.-J.; Yan, D.; Pei, Y.-B.; Zhao, L.; Li, Y.-B.; Wu, L.-B.; Jiang, J.-X.; Lai, G.-Q. The effect of graphene dispersion on the mechanical properties of graphene/epoxy composites. *Carbon* **2013**, *60*, 16-27.

(10) Yousefi, N.; Lin, X.; Zheng, Q.; Shen, X.; Pothnis, J. R.; Jia, J.; Zussman, E.; Kim, J.-K. Simultaneous in situ reduction, self-alignment and covalent bonding in graphene oxide/epoxy composites. *Carbon* **2013**, *59*, 406-417.

(11) Stankovich, S.; Dikin, D. A.; Dommett, G. H. B.; Kohlhaas, K. M.; Zimney, E. J.; Stach, E. A.; Piner, R. D.; Nguyen, S. T.; Ruoff, R. S. Graphene-based composite materials. *Nature* **2006**, *442*, 282-286.

(12) Stankovich, S.; Piner, R. D.; Nguyen, S. T.; Ruoff, R. S. Synthesis and exfoliation of isocyanate-treated graphene oxide nanoplatelets. *Carbon* **2006**, *44*, 3342-3347.

(13) Kim, H.; Abdala, A. A.; Macosko, C. W. Graphene/Polymer Nanocomposites. *Macromolecules* **2010**, *43*, 6515-6530.

(14) Tripathi, S. N.; Rao, G. S. S.; Mathur, A. B.; Jasra, R. Polyolefin/graphene nanocomposites: a review. *RSC Adv.* **2017**, *7*, 23615-23632.

(15) Stürzel, M.; Kempe, F.; Thomann, Y.; Mark, S.; Enders, M.; Mülhaupt, R. Novel Graphene UHMWPE Nanocomposites Prepared by Polymerization Filling Using Single-Site Catalysts Supported on Functionalized Graphene Nanosheet Dispersions. *Macromolecules* **2012**, *45*, 6878-6887.

(16) Tripathi, S. N.; Saini, P.; Gupta, D.; Choudhary, V. Electrical and mechanical properties of PMMA/reduced graphene oxide nanocomposites prepared via in situ polymerization. *J. Mater. Sci.* **2013**, *48*, 6223-6232.

(17) Park, S.; An, J.; Potts, J. R.; Velamakanni, A.; Murali, S.; Ruoff, R. S. Hydrazine-reduction

of graphite- and graphene oxide. *Carbon* **2011**, *49*, 3019-3023.

(18) Yan, D.-X.; Pang, H.; Li, B.; Vajtai, R.; Xu, L.; Ren, P.-G.; Wang, J.-H.; Li, Z.-M. Structured Reduced Graphene Oxide/Polymer Composites for Ultra-Efficient Electromagnetic Interference Shielding. *Adv. Funct. Mater.* **2015**, *25*, 559-566.

(19) Luo, Q.; Wei, P.; Huang, Q.; Gurkan, B.; Pentzer, E. B. Carbon Capsules of Ionic Liquid for Enhanced Performance of Electrochemical Double-Layer Capacitors. *ACS Appl. Mater. Interfaces* **2018**, *10*, 16707-16714.

(20) Song, N.-J.; Chen, C.-M.; Lu, C.; Liu, Z.; Kong, Q.-Q.; Cai, R. Thermally reduced graphene oxide films as flexible lateral heat spreaders. *J. Mater. Chem. A* **2014**, *2*, 16563-16568.

(21) Voiry, D.; Yang, J.; Kupferberg, J.; Fullon, R.; Lee, C.; Jeong, H. Y.; Shin, H. S.; Chhowalla, M. High-quality graphene via microwave reduction of solution-exfoliated graphene oxide. *Science* **2016**, *353*, 1413-1416.

(22) Wang, Y.; Shi, Z.; Yin, J. Facile Synthesis of Soluble Graphene via a Green Reduction of Graphene Oxide in Tea Solution and Its Biocomposites. *ACS Appl. Mater. Interfaces* **2011**, *3*, 1127-1133.

(23) Hou, D.; Liu, Q.; Cheng, H.; Li, K.; Wang, D.; Zhang, H. Chrysanthemum extract assisted green reduction of graphene oxide. *Mater. Chem. Phys.* **2016**, *183*, 76-82.

(24) Bo, Z.; Shuai, X.; Mao, S.; Yang, H.; Qian, J.; Chen, J.; Yan, J.; Cen, K. Green preparation of reduced graphene oxide for sensing and energy storage applications. *Sci. Rep.* **2014**, *4*, 4684.

(25) Alsharaeh, E. H.; Faisal, N. H.; Othman, A. A.; Ahmed, R. Evaluation of Nanomechanical Properties of (Styrene–Methyl Methacrylate) Copolymer Composites Containing Graphene Sheets. *Ind. Eng. Chem. Res.* **2013**, *52*, 17871-17881.

(26) Kuilla, T.; Bhadra, S.; Yao, D.; Kim, N. H.; Bose, S.; Lee, J. H. Recent advances in

graphene based polymer composites. *Prog. Polym. Sci.* **2010**, *35*, 1350-1375.

(27) Alsharaeh, E. H.; Othman, A. A.; Aldosari, M. A. Microwave Irradiation Effect on the Dispersion and Thermal Stability of RGO Nanosheets within a Polystyrene Matrix. *Materials (Basel)* **2014**, *7*, 5212-5224.

(28) Aldosari, M. A.; Othman, A. A.; Alsharaeh, E. H. Synthesis and Characterization of the in Situ Bulk Polymerization of PMMA Containing Graphene Sheets Using Microwave Irradiation. *Molecules* **2013**, *18*, 3152-3167.

(29) Polshettiwar, V.; Varma, R. S. Microwave-Assisted Organic Synthesis and Transformations using Benign Reaction Media. *Acc. Chem. Res.* **2008**, *41*, 629-639.

(30) Kempe, K.; Becer, C. R.; Schubert, U. S. Microwave-Assisted Polymerizations: Recent Status and Future Perspectives. *Macromolecules* **2011**, *44*, 5825-5842.

(31) Zhu, J.; Zhu, X.; Zhang, Z.; Cheng, Z. Reversible addition–fragmentation chain transfer polymerization of styrene under microwave irradiation. *J. Polym. Sci. A* **2006**, *44*, 6810-6816.

(32) Stange, H.; Ishaque, M.; Niessner, N.; Pepers, M.; Greiner, A. Microwave-Assisted Free Radical Polymerizations and Copolymerizations of Styrene and Methyl Methacrylate. *Macromol. Rapid Commun.* **2006**, *27*, 156-161.

(33) Zofchak, E. S.; LaNasa, J. A.; Mei, W.; Hickey, R. J. Polymerization-Induced Nanostructural Transitions Driven by In Situ Polymer Grafting. *ACS Macro Lett.* **2018**, *7*, 822-827.

(34) Chen, Q.; Shen, Y.; Zhang, S.; Zhang, Q. M. Polymer-Based Dielectrics with High Energy Storage Density. *Annu. Rev. Mater. Res.* **2015**, *45*, 433-458.

(35) Zhu, L. Exploring Strategies for High Dielectric Constant and Low Loss Polymer Dielectrics. *J. Phys. Chem. Lett.* **2014**, *5*, 3677-3687.

(36) Brooks, W. L. A.; Sumerlin, B. S. Microwave-Assisted RAFT Polymerization. *Isr. J. Chem.*

2012, *52*, 256-263.

(37) Brown, S. L.; Rayner, C. M.; Graham, S.; Cooper, A.; Rannard, S.; Perrier, S. Ultra-fast microwave enhanced reversible addition-fragmentation chain transfer (RAFT) polymerization: monomers to polymers in minutes. *Chem. Commun.* **2007**, 2145-2147.

(38) Li, J.; Zhu, X.; Zhu, J.; Cheng, Z. Microwave-assisted nitroxide-mediated miniemulsion polymerization of styrene. *Radiat. Phys. Chem.* **2007**, *76*, 23-26.

(39) Li, J.; Zhu, X.; Zhu, J.; Cheng, Z. Microwave-assisted nitroxide-mediated radical polymerization of styrene. *Radiat. Phys. Chem.* **2006**, *75*, 253-258.

(40) Uyor, U. O.; Popoola, A. P.; Popoola, O.; Aigbodion, V. S. Energy storage and loss capacity of graphene-reinforced poly(vinylidene fluoride) nanocomposites from electrical and dielectric properties perspective: A review. *Adv. Polym. Tech.* **2018**, *37*, 2838-2858.

(41) Wang, D.; Bao, Y.; Zha, J.-W.; Zhao, J.; Dang, Z.-M.; Hu, G.-H. Improved Dielectric Properties of Nanocomposites Based on Poly(vinylidene fluoride) and Poly(vinyl alcohol)-Functionalized Graphene. *ACS Appl. Mater. Interfaces* **2012**, *4*, 6273-6279.

(42) Wang, D.; Zhang, X.; Zha, J.-W.; Zhao, J.; Dang, Z.-M.; Hu, G.-H. Dielectric properties of reduced graphene oxide/polypropylene composites with ultralow percolation threshold. *Polymer* **2013**, *54*, 1916-1922.

(43) Li, H.; Chen, Z.; Liu, L.; Chen, J.; Jiang, M.; Xiong, C. Poly(vinyl pyrrolidone)-coated graphene/poly(vinylidene fluoride) composite films with high dielectric permittivity and low loss. *Compos. Sci. Technol.* **2015**, *121*, 49-55.

(44) Malas, A.; Bharati, A.; Verkinderen, O.; Goderis, B.; Moldenaers, P.; Cardinaels, R. Effect of the GO Reduction Method on the Dielectric Properties, Electrical Conductivity and Crystalline Behavior of PEO/rGO Nanocomposites. *Polymers* **2017**, *9*, 613.

(45) Zhang, G.; Li, Y.; Tang, S.; Thompson, R. D.; Zhu, L. The Role of Field Electron Emission in Polypropylene/Aluminum Nanodielectrics Under High Electric Fields. *ACS Appl. Mater. Interfaces* **2017**, *9*, 10106-10119.

(46) Zhang, G.; Brannum, D.; Dong, D.; Tang, L.; Allahyarov, E.; Tang, S.; Kodweis, K.; Lee, J.-K.; Zhu, L. Interfacial Polarization-Induced Loss Mechanisms in Polypropylene/BaTiO3 Nanocomposite Dielectrics. *Chem. Mater.* **2016**, *28*, 4646-4660.

(47) Li, J.; Claude, J.; Norena-Franco, L. E.; Seok, S. I.; Wang, Q. Electrical Energy Storage in Ferroelectric Polymer Nanocomposites Containing Surface-Functionalized BaTiO3 Nanoparticles. *Chem. Mater.* **2008**, *20*, 6304-6306.

(48) Lin, X.; Hu, P.; Jia, Z.; Gao, S. Enhanced electric displacement induces large energy density in polymer nanocomposites containing core–shell structured BaTiO3@TiO2 nanofibers. *J. Mater. Chem. A* **2016**, *4*, 2314-2320.

(49) Wu, C.; Huang, X.; Xie, L.; Wu, X.; Yu, J.; Jiang, P. Morphology-controllable graphene–TiO2 nanorod hybrid nanostructures for polymer composites with high dielectric performance. *J. Mater. Chem.* **2011**, *21*, 17729-17736.

(50) Hummers, W. S.; Offeman, R. E. Preparation of Graphitic Oxide. *J. Am. Chem. Soc.* **1958**, *80*, 1339-1339.

(51) Dreyer, D. R.; Park, S.; Bielawski, C. W.; Ruoff, R. S. The chemistry of graphene oxide. *Chem. Soc. Rev.* **2010**, *39*, 228-240.

(52) Rieger, J. The glass transition temperature of polystyrene. *J. Therm. Anal.* **1996**, *46*, 965-972.

(53) *Broadband Dielectric Spectroscopy*; Springer, Berlin, Heidelberg: New York, 2003.

(54) Choi, U. H.; Colby, R. H. The Role of Solvating 12-Crown-4 Plasticizer on Dielectric

Constant and Ion Conduction of Poly(ethylene oxide) Single-Ion Conductors. *Macromolecules* **2017**, *50*, 5582-5591.

(55) Choi, U. H.; Liang, S.; Chen, Q.; Runt, J.; Colby, R. H. Segmental Dynamics and Dielectric Constant of Polysiloxane Polar Copolymers as Plasticizers for Polymer Electrolytes. *ACS Appl. Mater. Interfaces* **2016**, *8*, 3215-3225.

(56) Thakur, Y.; Zhang, T.; Iacob, C.; Yang, T.; Bernholc, J.; Chen, L. Q.; Runt, J.; Zhang, Q. M. Enhancement of the dielectric response in polymer nanocomposites with low dielectric constant fillers. *Nanoscale* **2017**, *9*, 10992-10997.

(57) Qi, L.; Petersson, L.; Liu, T. Review of Recent Activities on Dielectric Films for Capacitor Applications. *J. Int. Counc. Electr. Eng.* **2014**, *4*, 1-6.

TOC